RELAXATION POLARIZATION DEPENDENCE OF CIRCULAR VECTOR GRATINGS IN AZOBENZENE MOLECULAR GLASSY FILMS

A.Ozols, P.Augustovs, K.Traskovskis, V.Kokars,
L.Laipniece, A.Ruduss, K.Balodis

Faculty of Materials Science and Applied Chemistry, Riga Technical University

1. Motivation

1) As is well known, efficiency and properties of holographic recording in azobenzene-based materials strongly depend on the recording beam light polarizations. The first and the main goal of this study was to investigate the dependence of grating **relaxation processes** on the readout beam polarization.

2) The second goal was to find the holographic parameters of the azobenzene molecular films recently synthesized at the Faculty of Materials Science and Applied Chemistry, Riga Technical University, and to evaluate the results of sample structure.

3) The third goal was to reveal the grating recording and relaxation peculiarities in so called “sandwich” type samples compared to ordinary samples of the same chemical structure .

3. Samples

Four types of molecular films containing azobenzne chromophores have been studied:

1) KT-38, synthesized by Kaspars Traskovskis,
2) AR-173, synthesized by Armands Rudušs,
3) B-21, synthesized by Kārlis Balodis,
4) LL-75, synthesized by Lauma Laipniece.

Next the information about the samples.

KT-38

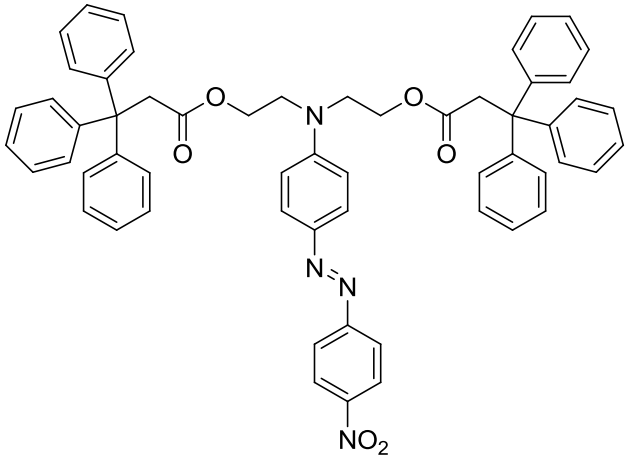

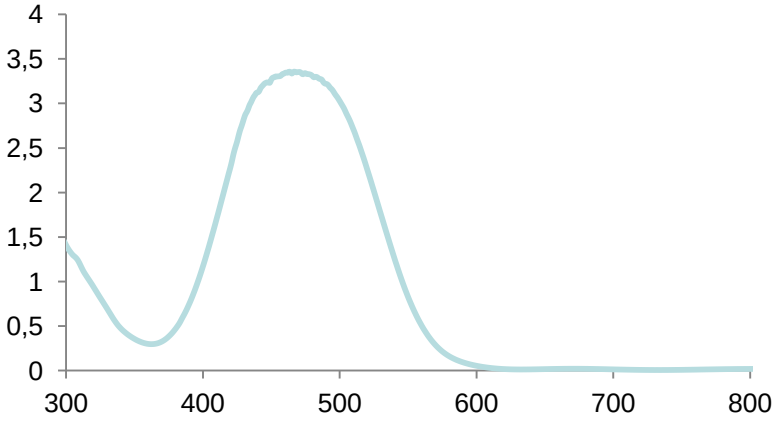

Absorption spectrum of KT-38 film.

KT-38=((4-((4-Nitrophenyl)diazenyl)phenyl)azanediyl)bis(ethane-2,1-diyl) bis(3,3,3-triphenylpropanoate).

KT-38 is composed of well-known azodye core, Disperse Red 1 (DR1) and 3,3,3-triphenylpropionic acid (tPh) as a glass-formation promoting group.

(NH_2 - donor group, NO_2 –acceptor group).

AR-173

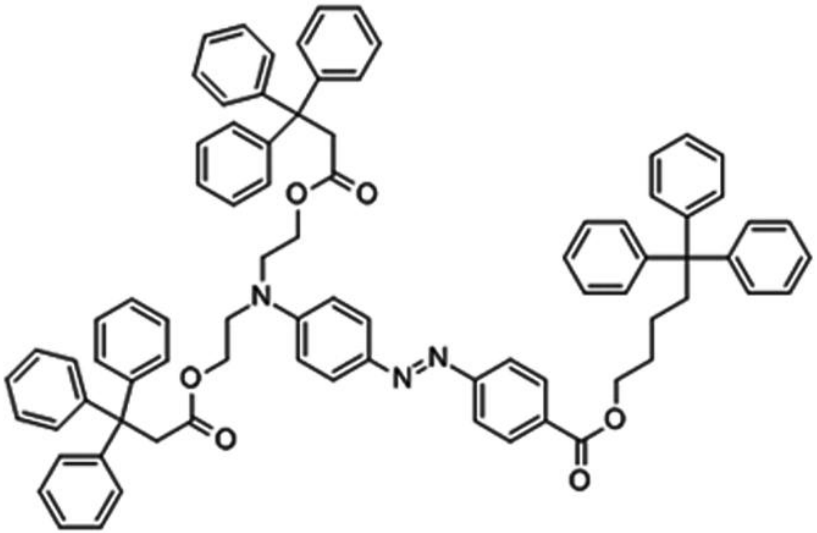

AR-173 = (E)-((4-((4-(((5,5,5-triphenylpentyl)oxy)carbonyl)phenyl)diazenyl) phenyl)azanediyl)bis(ethane-2,1-diyl) bis(3,3,3-triphenylpropanoate).

is composed of well-known azodye core and para-Methyl Red, and 3,3,3-triphenylpropionic acid as a glass-formation promoting group. Besides, an additional 5,5,5-triphenylpentyl group was introduced to the electron acceptor part of the molecule in order to additionally reduce possible chromophore interactions in solid-phase. [NH_2-D, CHO-A].

B-21

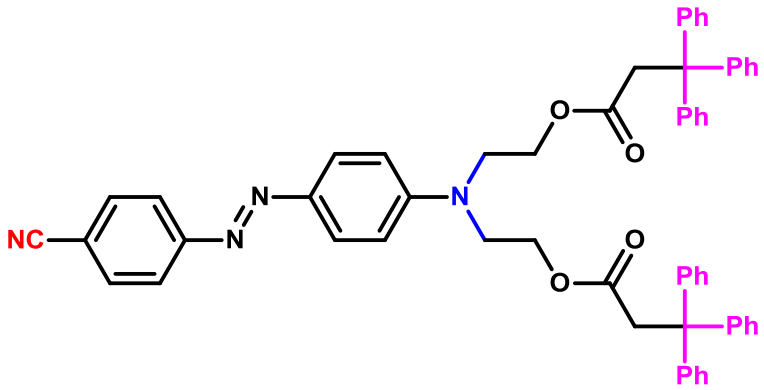

B-21=((4-((4-cyanophenyl)diazenyl)phenyl)azanediyl)bis(ethane-2,1-diyl) bis(3,3,3-triphenylpropanoate).

Red – cyano group (electron acceptor)

Blue – dialkylamino group (electron donor)

Violet – triphenylgroups of large spatial size promoting formation of thin transparent films from volatile nonpolar organic solvents.

LL-75

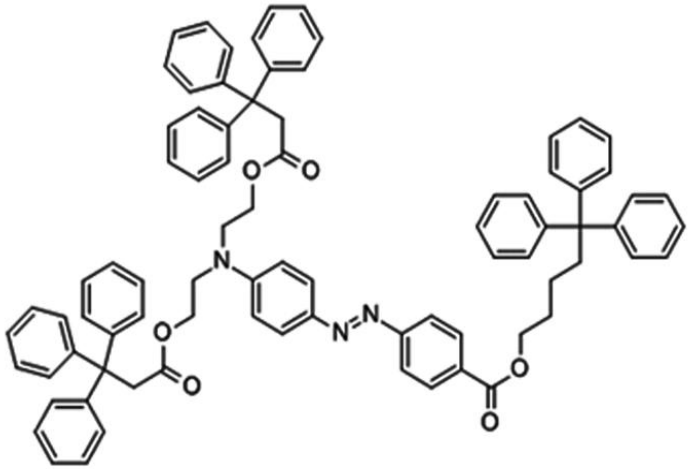

LL-75=4'-(*N*-(2-[3,5-dibenzyloxybenzoyloxy]ethyl)-*N*-methylamino)-2-(2-[3,5-dibenzyloxybenzoyloxy]ethoxy)-4-nitroazobenzene.

Film with *dendronized* azobenzene chromophore. (NH_2 – D, CHO –A).

Absorption spectra

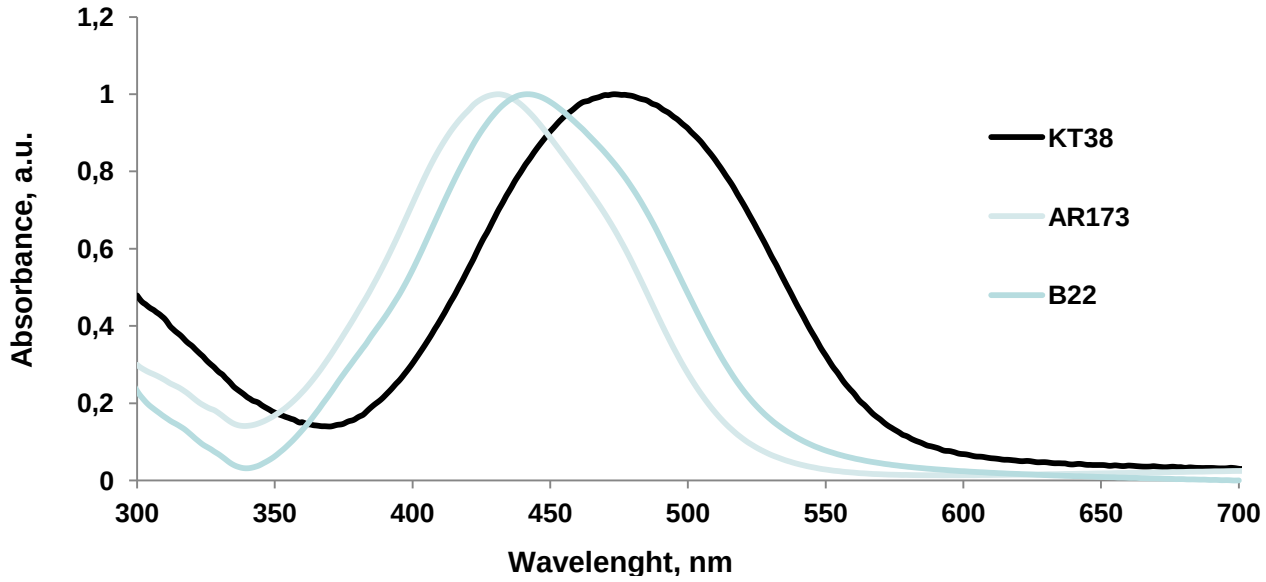

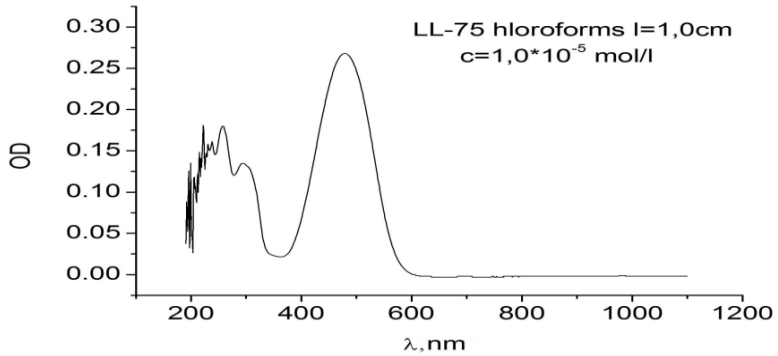

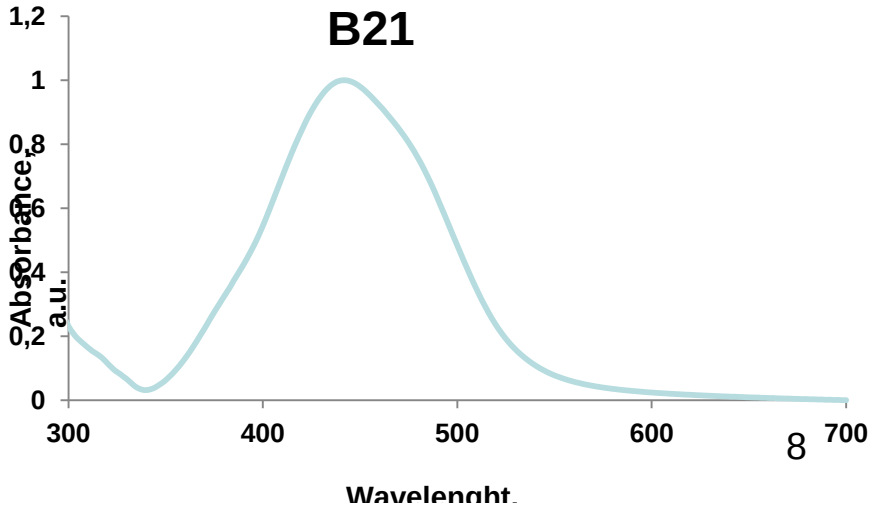

3. Experiments

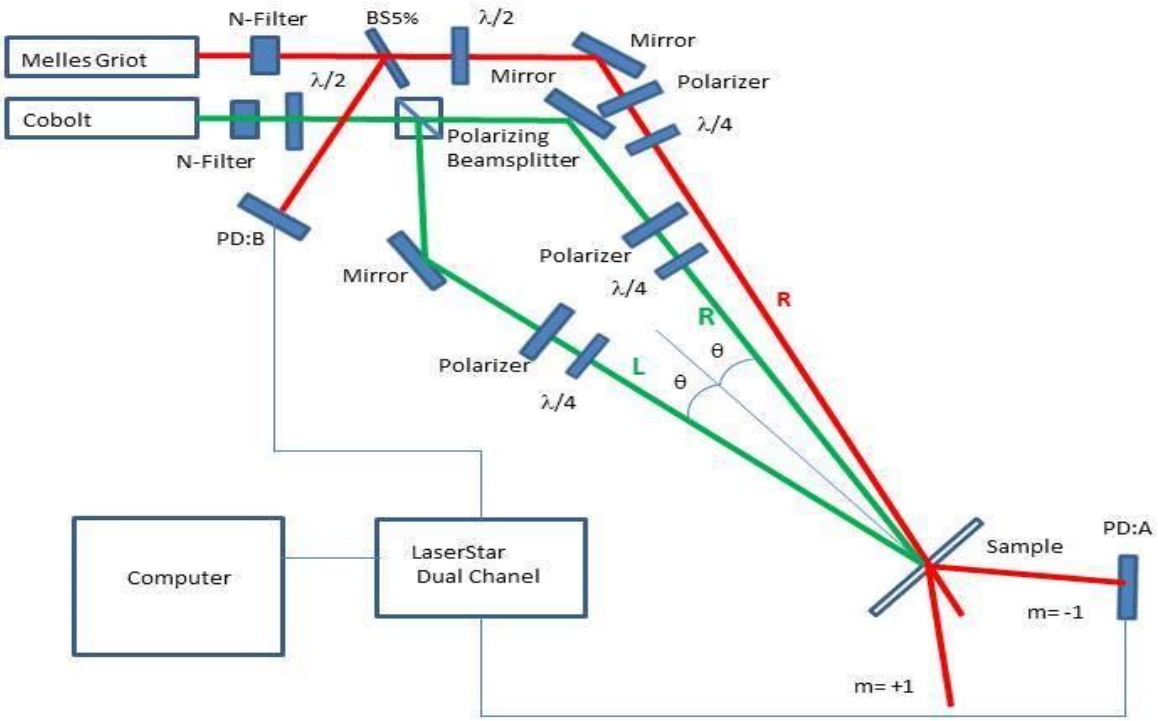

Fig.1. Experimental setup.

Vector grating recording was performed with green circular orthogonally polarized *L* un *R* beams at 532 nm whereas their readout was made by red either *R*- or *L*-polarized beam at 632.8 nm. After the recording diffraction efficiency (DE) relaxation was measured by attenuated (0.44 mW) 632.8 nm beam. Grating periods were Λ = 0.50, 2.0 and 7.0 μm.

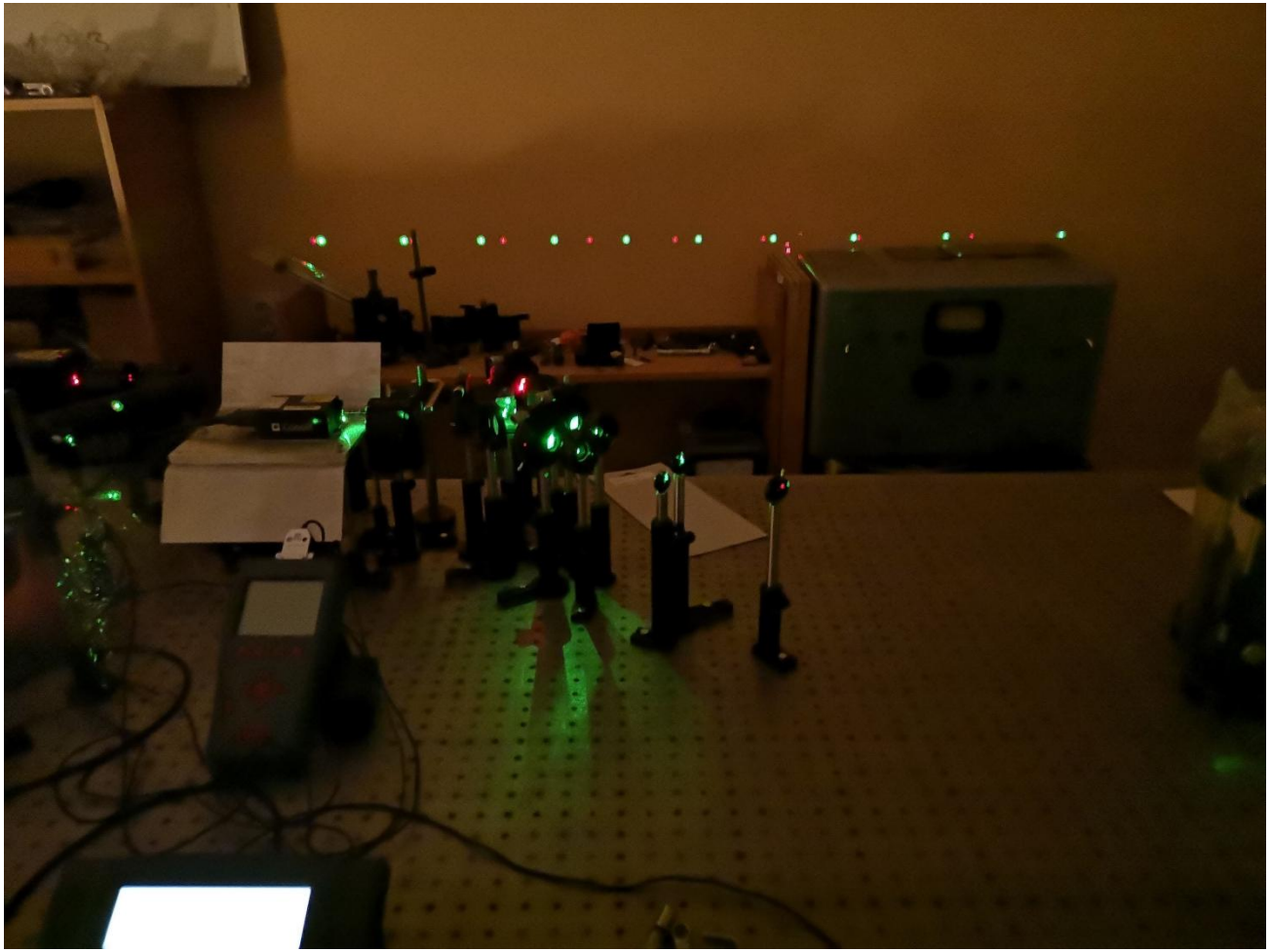

Experimental setup view. Many diffraction orders on reflection are seen on the wall at Λ = 7.0μm. The same on transmission (not seen here).

4.Holographic characteristics

Table 4.1. Λ= 0.50μm, I=0.32 W/cm^2

Sample, readout conditions	t , s	DE,%	W, J/cm^2%	REF, (%cm)^2/J	DE decay time 50%, s
AR-173, readout by *R*- polarization	128	2,4	17,50	0,14	∞
AR-173, readout by *R*- polarization, short exposure	29	2,1	4,4	0,48	>660
AR-173, readout by *L*- polarization	525	0,32	520	0,0006	∞
KT-38, readout by *R*- polarization	240	9,1	8,4	1,08	∞
KT-38, readout by *R*- polarization, short exposure	15	4,1	1,2	3,5	25
KT-38, readout by *L*- polarization	240	6,1	13	0,49	∞

Sample, readout conditions	*t*, s	DE,%	*W*, J/cm^2 %	REF, (%cm)^2/J	DE decay time 50%, s
LL-75, readout by *R*- polarization	134	1,7	25	0,071	∞
LL-75, readout by *R*- polarization, short exposure	10	1,4	2,3	0,6	4,1
LL-75, readout by *L*- polarization	477	0,87	176	0,0050	∞
B-21, readout by *R*- polarization	285	4,4	21	0,21	∞
B-21, readout by *R*- polarization, short exposure	7	1,8	1,3	1,4	44
B-21, readout by *L*- polarization	285	3,9	23	0,17	∞

At large exposures (>100s) no decay took place at all (except “sandwiches”). The same also at short exposures by readout with *L*-polarization. DE decay was significant when read out by *R*-polarization. It is seen also from Table 4.1 that readout by *R*-polarization is much more efficient than by *L*-polarization and the best sample is KT-38. Relaxation is the slowest in AR-173 samples.

Table 4.2. λ=2.0μm, I=0.30 W/cm^2

Sample, readout conditions	t ,s	DE,%	W, J/cm^2%	REF, (%cm)^2/J	DE decay time 50%, s
AR-173, readout by - R polarization	588	18	9,6	1,9	∞
AR-173, readout by L- polarization	588	17	10	1,7	∞
AR-173, readout by R- polarization, short exposure	25	2,2	3,5	0,6	> 720
B-21, readout by R- polarization	111	26	1,3	20	∞
B-21, readout by L- polarization	105	26	1,2	22	∞
B-21, readout by R- polarization, short exposure	3,2	2,2	0,43	5,1	35

Sample, readout conditions	*t* ,s	DE,%	W, J/cm^2%	REF, (%cm)^2/J	DE decay time 50%, s
KT-38, readout by *R*- polarization	86	26	0,99	26	20
KT-38, readout by *L*- polarization	85	24	1,0	24	∞
KT-38, readout by *R*- polarization, short exposure	5,1	3,9	0,39	10	20
LL-75, readout by *R*- polarization	255	28	2,7	10	∞
LL-75, readout by *L*- polarization	291	28	3,1	8,8	∞
LL-75, readout by *R*- polarization, short exposure	5	1,6	0,95	1,65	3,5

Conclusions from Table 4.2:

1) Readout by *R*-polarization is the most efficient (except B-21 sample in which difference is small);

2) KT-38 sample again is the most efficient;

3) Again relaxation is the slowest in AR-173 sample .

Table 4.3. *Sandwich* type samples, Λ=2.0μm, I=0.32 W/cm^2 , readout by *R*-polarization.

Sample	*t*, s	DE,%	*W*, J/cm^2%	REF, (%cm)^2/J
KT-38_b_snd	492	11	14	0,77
KT-38_b_snd , short exposure	4,9	3,6	0,44	8,1
AR-173_b_snd	444	81	1,8	46
AR-173_b_snd, short exposure	4,8	6,8	0,23	29

It is clearly seen that sandwiched AR-173 sample is much more efficient than ordinary AR-173 sample (REF=46>>REF=1.9). The highest **DE=81%** is achieved.

On the contrary, sandwiched KT-38 sample is considerably less efficient than ordinary KT-38 sample (REF=8.1<REF=26).

Table 4.4. Λ= 7.0μm, I=0.32 W/cm^2

Sample, readout conditions	*t*,*s*	DE,%	*W*, J/cm^2%	REF, (%cm)^2/ J	DE decay time 50%, s
AR-173, readout by - *R* polarization	378	29	4,2	7,0	∞
AR-173, readout by *R*- polarization, short exposure	20	3,3	1,9	1,7	>720
AR-173, readout by *L*- polarization	387	27	4,5	6,0	∞
KT-38, readout by - *R* polarization	134	28	1,5	18	∞
KT-38, readout by *R*- polarization, short exposure	5	3,8	0,42	9,1	15
KT-38, readout by *L*- polarization	136	26	1,7	15	∞

Sample, readout conditions	*t*,*s*	DE,%	*W*, J/cm^2%	REF, (%cm)^2/ J	DE decay time 50%, s
LL-75, readout by - *R* polarization	402	24	5,4	4,5	∞
LL-75, readout by *R*- polarization, short exposure	10	1,8	1,8	1,0	4
LL-75, readout by *L*- polarization	410	26	5,1	5,1	∞
B-21, readout by *R*- polarization	117	29	1,3	22	∞
B-21, readout by *R*- polarization, short exposure	3	2,3	0,41	5,6	34
B-21, readout by *L*- polarization	115	27	1,3	20	∞

Conclusions from Table 4.4:

1)Again (except LL-75) readout by *R*-polarization is the most efficient .

2) Again grating decay is the slowest in AR-173 sample.

3) In this case the most efficient sample was B-21.

From the above results the question arises: how is it possible that gratings decay when read out by *R*- polarization but do not decay by *L* – polarization? Answer can be obtained from DE kinetics.

5. Grating relaxation peculiarities

Further we shall illustrate the following peculiarities of *L*-*R* grating relaxation in azobenzene chromophore-based organic molecular films using DE kinetic curves (DE versus exposure time curves).

1) *There is no grating relaxation after reaching DE maximum.*

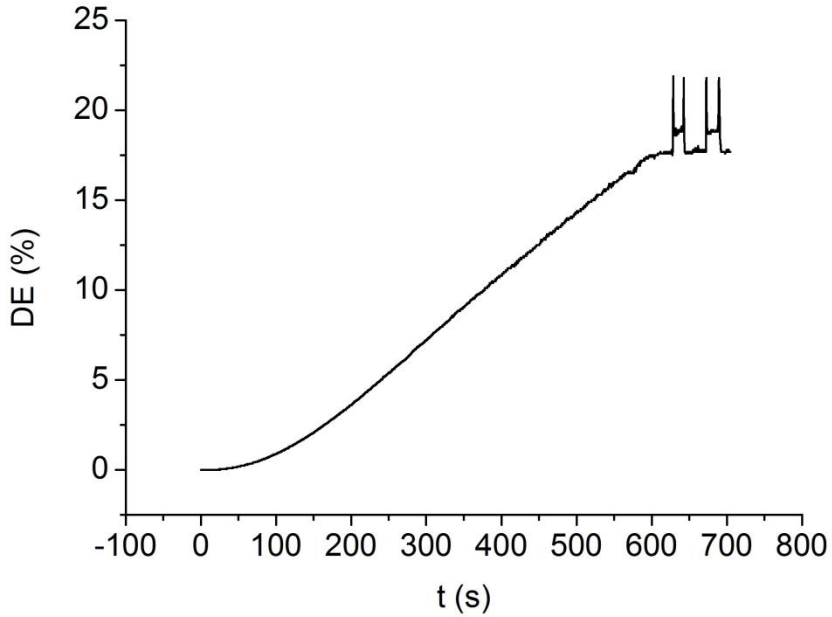

Fig.2. Sample AR-173, readout by *L*-polarization , Λ= 2.0μm. Two pulse-like increments are due to the temporary switch to the readout by *R*-polarization. Four spikes are due to the rotation of $\lambda/4$ plate. Analogously further.

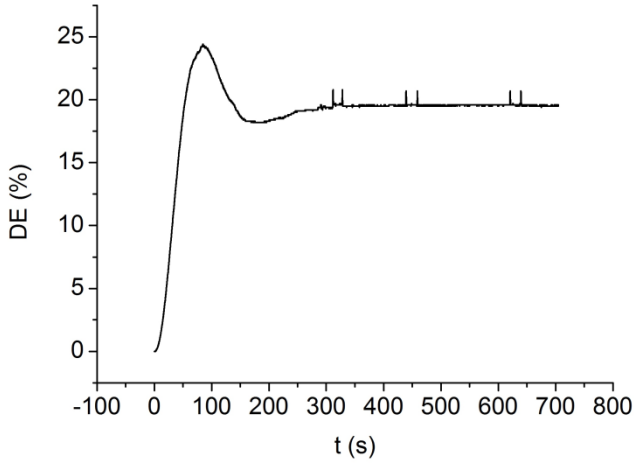

Fig.3. Sample KT-38, readout by *L*-polarization, Λ= 2.0μm.

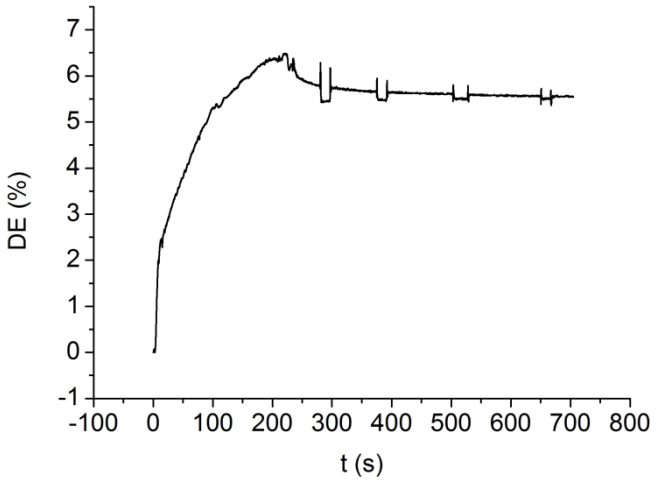

Fig.4. Sample KT-38, readout by *R*-polarization, Λ= 0.5μm .

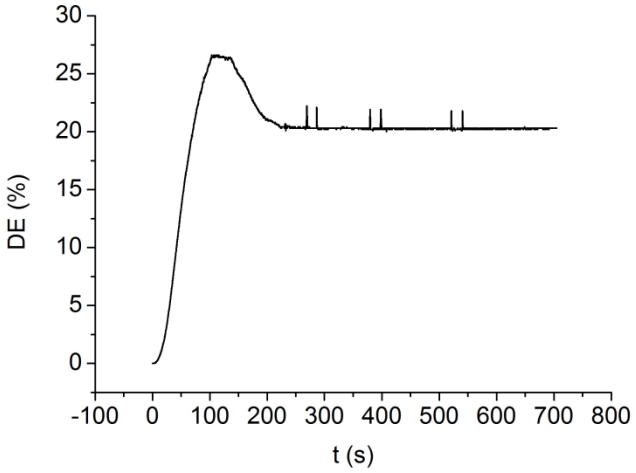

Fig.5. Sample B-21, readout by L-polarization, Λ= 2.0μm .

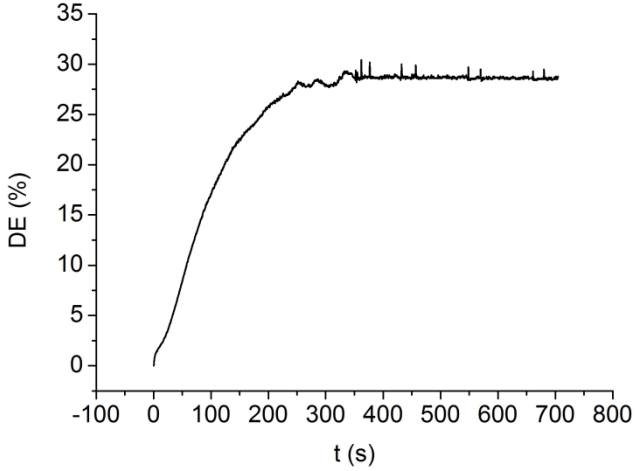

Fig.6. Sample LL-75, readout by R-polarization, Λ= 2.0μm.

2) *After a short exposure*, DE decay takes place when read out by *R*-polarization whereas very low DE values are read out by *L*-polarization.

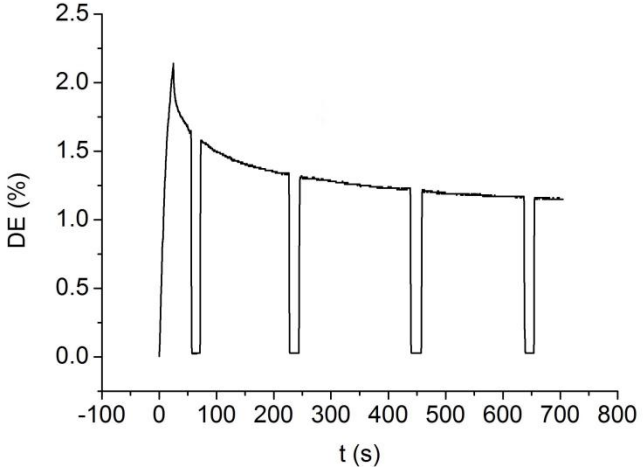

Fig.7. Sample AR-173, Λ= 2.0μm.

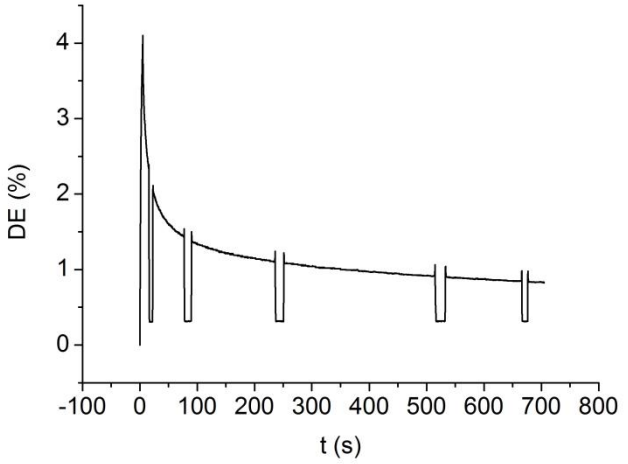

Fig.8. Sample KT-38, Λ= 2.0μm.

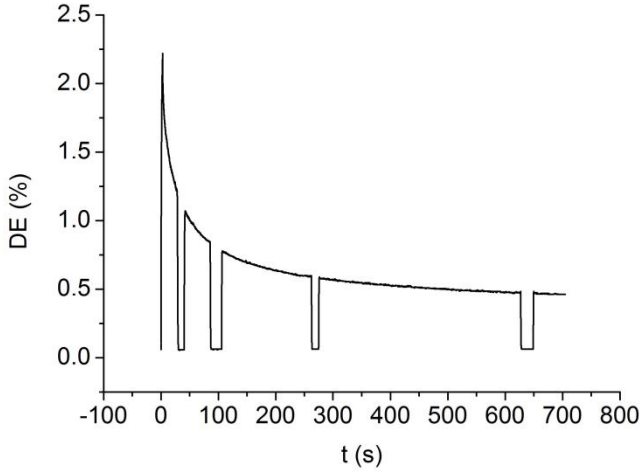

Fig.9. Sample B-21, Λ= 2.0μm.

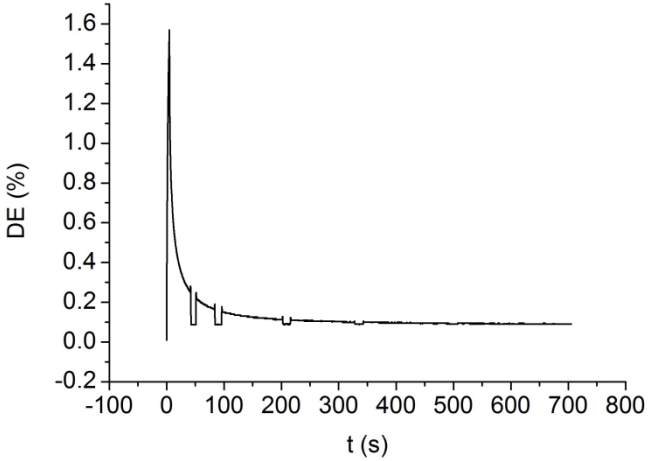

Fig.10. Sample LL-75, Λ= 2.0μm.

3) *After a short exposure* no decay takes place when read out by *L*-polarization.

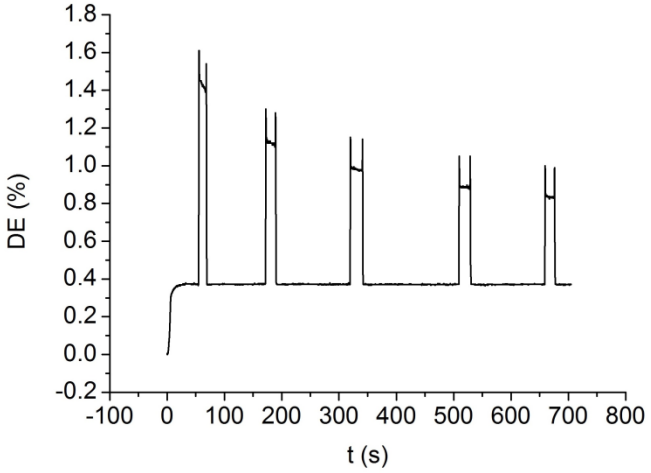

Fig.11. Sample KT-38, Λ= 2.0μm.

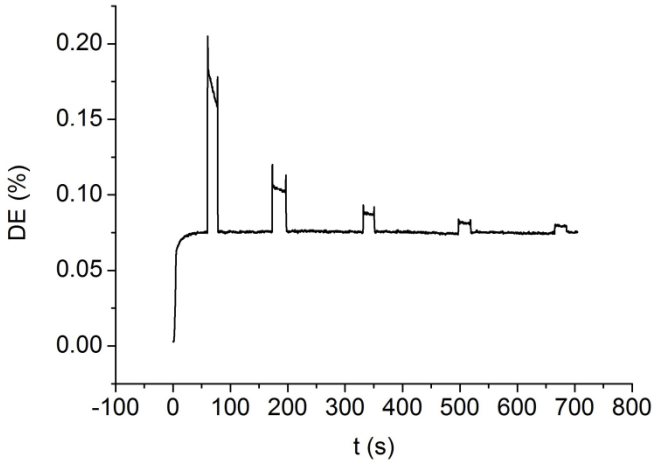

Fig.12. Sample LL-75, Λ= 2.0μm

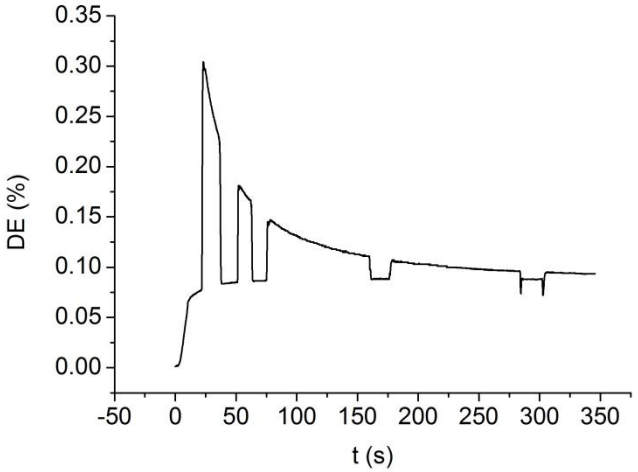

Fig.13. Sample LL-75, Λ= 0.5μm.

Figures 11-13 clearly show that DE decays by *R*-polarization but does not decay by *L*-polarization.

4) *In sandwich- type samples*, DE decays by *R*-polarization whereas by *L*-polarization DE=const=0.

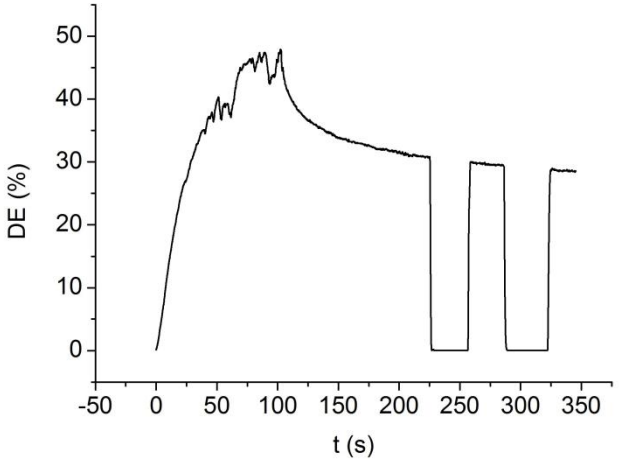

Fig.14. Sample AR-173_b_snd, Λ= 2.0μm.

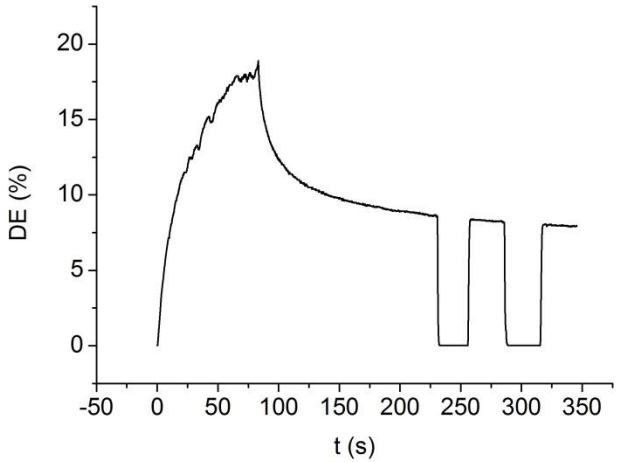

Fig.15. Sample KT-38_b_snd, Λ= 2.0μm.

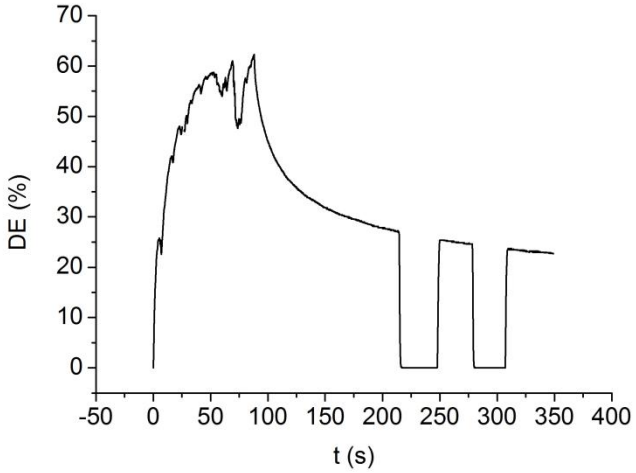

Fig.16. Sample B-21_snd_plns, Λ= 2.0μm.

6. Grating period dependence of decay (relaxation) time.

Sample, Λ=0.5μm	AR-173	B-21	KT-38	LL-75
Decay time 50%, s	>660	44	25	4.1

Sample, Λ=2.0μm	AR-173	B-21	KT-38	LL-75
Decay time 50%, s	>720	35	20	10

Sample, Λ=7.0μm	AR-173	B-21	KT-38	LL-75
Decay time 50%, s	>720	34	15	4.0

[Sandwich type samples AR-173 and KT-38 at Λ=2.0μm have the same decay times as ordinary ones]. It is seen that decay times decrease in the sample sequence: AR-173, B-21, KT-38 and LL-75. There is a certain tendency of decay time decrease with a grating period.

7. Discussion

The following 4-step model can explain the observed peculiarities of DE kinetics:

1. Charge transfer takes place over the aromatic core bridge from donors to acceptors under the influence of 532 nm recording light. As the result, the chromophore molecules which initially were in the *trans* state turn to the *cis* state acquiring the electric dipole moment and reorienting perpendicularly to the electric vector of light.
2. Further *trans*-*cis*-*trans* photoisomerization cycles takes place according to the spatial polarization modulation of recording light leading to the inscription of volume birefringence grating (VBG).
3. VBG creates also spatially modulated photoisomerization pressure , electric gradient force and mass transfer resulting in surface relief grating (SRG) and/or volume density grating (VDG) recording.
4. At first, VBG is recorded, and it decays during the readout. The following SRG and VDG grow slower but are stable. There are only SRG and DG at saturation.

Thus our experiments confirm the hypothesis of Jeļena Miķelsone (PhD thesis-2018) that VBG is the necessary prerequisite of SRG (and DG) formation.

Our experiments (by grating recording from film and glass substrate sides and AFM) have shown that no SRG are forming in sandwich -type samples. Only VBG and DG can be recorded in these samples.

On the other hand, DE relaxation experiments with the circular readout polarization change to the opposite one in sandwich type samples have shown that **only VBG** are recorded since DE=0 by readout with *L*-polarization (slide 22). As is known, only in the case of VBG there is only one first-order diffraction maximum which switches to the symmetric first-order position when the readout polarization is switched to the orthogonal circular one [L.Nikolova and P.S.Ramanujam, Polarization Holography, 2009].

.

Sandwich type sample AR-173 , as previously shown, was the most efficient with DE up to 81%. We have just proved that this was the result of efficient VBG recording. Evidently, this is due to the additional triphenylgroup (slide No5) enabling additional isolation of chromophore group. Therefore, such samples can be used in dynamic holography as already shown by our common holographic light amplification experiments with prof. S.Odoulov's group in Kiev, Institute of Physics, National Academy of Sciences, Ukraine.

However, *ordinary* AR-173 sample is not the most efficient. (Far from that as we shall see at the next slide). Besides, it has the highest decay time (>11 min.), which can be explained by the existence of the additional triphenylgroups making chromophores more bulky. It seems that efficient formation of SRG and DG hampers the formation of VBG. Yet, this point deserves further investigation.

Ordinary samples can be ranged in the following way by recording efficiency factor REF.

Λ= 0.5μm: KT-38, B-21, AR-173, LL-75

Λ= 2.0μm: KT-38, B-21, LL-75, AR-173

Λ= 7.0μm: B-21, KT-38, AR-173, LL-75.

DE had a tendency to *increase* when the grating period was increased. This can be explained by the decrease of the *scalar component* of the grating. Even with orthogonal circular polarizations there is a small scalar component (additional light intensity modulation) in the recording light spatial distribution because of polarization *ellipticity* caused by non-zero incident angle. This scalar component decreases when the grating period is increased. (interference pattern visibility V = 0.28, 0.018 and 0.0014, respectively).

Grating decay time had a tendency to *decrease* when the grating period was increased. Most probably, this is due to the surface *tension decrease* preventing mass transfer . As known, surface tension changes are inversely proportional to the grating period [A.Ozols et al, J.Appl.Phys.1994].

Grating decay times *decrease* for all periods in the sample sequence : AR-173, B-21, KT-38, LL-75. Obviosly, this sample arrangement is determined by the bulkiness of their structures. Larger structure bulkiness leads to larger decay time. Thus sample AR-173 contains three triphenylgroups, samples B-21 and KT-38 contain two triphenylgroups each, denronized azobenzene chromophore LL-75 contains only pentylgroups.

8. Conclusions

1) Circular vector grating recording and relaxation is experimentally studied in different azobenzene-based molecular films.

2) Diffraction efficiency as high as 81% was achieved in sandwich -type sample AR-173. We believe that this is due to the additional triphenylgroups enabling additional isolation of chromophore group.

3) The observed grating relaxation peculiarities are explained by initial volume birefringence grating (VBG) recording followed by surface relief grating (SRG) and volume density grating (VDG) recording. *In our experimental setup*, *R*- polarization "feels" all three gratings whereas *L*-polarization "feels"only SRG and DG. At large exposures SRG and VDG dominate.

.

4) In sandwich-type samples only VBG are recorded.

5) Diffraction efficiency has a tendency to increase when the grating period is increased. This tendency is explained by the decrease of the *scalar component* of the grating.

6) Grating decay time has a tendency to decrease when the grating period was increased. Evident reason is the surface tension decrease preventing mass transfer.

.

7) Grating decay times decrease for all periods in the sample sequence : AR-173, B-21, KT-38, LL-75. This sample arrangement is determined by the bulkiness of their structures.

THANK YOU FOR ATTENTION!